Received: 4 June 2018 | Revised: 14 July 2018 | Accepted: 17 July 2018

DOI: 10.1002/rra.3346

RESEARCH ARTICLE

WILEY

Three-dimensional numerical simulations of smooth, asymmetrically roughened, and baffled culverts for upstream passage of small-bodied fish

Gangfu Zhang[1,2] | Hubert Chanson[1]

[1] School of Civil Engineering, The University of Queensland, Brisbane, Queensland, Australia

[2] Resources East, WSP Australia Pty Limited, Brisbane, Queensland, Australia

Correspondence
Gangfu Zhang, Professional Water Resources Engineer, Resources East, WSP Australia Pty Limited, Brisbane, QLD 4000, Australia.
Email: gangfu.zhang@wsp.com; gangfu.zhang@uqconnect.edu.au

Present Address
Gangfu Zhang, Resources East, WSP Australia Pty Limited, Brisbane, QLD 4000, Australia.

Funding information
Australian Research Council, Grant/Award Number: LP140100225

Abstract

Traditional box culvert designs lead to development of high velocity zones in the culvert barrel that often impede upstream migration of fish. Herein, three-dimensional Reynolds-averaged Navier-Stokes (RANS)- and Large eddy simulation (LES)-based computational fluid dynamics (CFDs) simulations were performed to compare the effectiveness of smooth, asymmetrically roughened, and corner-baffled barrels, in creating low-velocity zones (LVZs) and providing opportunity for upstream passage of small-bodied fish. The results revealed distinctive benefits provided by the asymmetrically roughened and corner-baffled barrels relative to the smooth barrel. Cross-sectional asymmetry, corners, and obstructions are important factors that contribute to the generation of LVZs conducive to fish passage, albeit contiguity of LVZs is required, particularly for weak swimmers. The study demonstrates the adequacy and effectiveness of CFD models to complement traditional laboratory studies in understanding basic mechanisms beneficial to fish passage and to provide insights into future designs.

KEYWORDS

box culverts, CFD numerical modelling, fish passage, hydraulic structures, low-velocity zones, small-bodied fish

1 | INTRODUCTION

A culvert is a relatively short hydraulic conduit designed to pass floodwater through an embankment. The optimum engineering designs typically require the smallest barrel size compatible with an inlet control operation at design flow conditions (Chanson, 2000, 2004; Herr & Bossy, 1965). For design and less-than-design discharges, the engineering optimization leads to large barrel velocities, which might prevent upstream fish passage during rainfall and run-off events (Behlke, Kane, Mcleen, & Travis, 1991). Small-bodied freshwater fish species are especially affected, as their characteristic endurance speed of less than 0.6 m/s could remain well below design flow velocities (Hurst, Kay, Ryan, & Brown, 2007; Rodgers et al., 2014).

Recent recognitions of the ecological impacts of culverts on fish passage led to reconsiderations of culvert design guidelines (Behlke et al., 1991; Chorda, Larinier, & Font, 1995; Hotchkiss & Frei, 2007). Roughness-induced effects on fish swimming performance were investigated in a number of recent studies (Baki, Zhu, & Rajaratnam, 2014; Cassan, Tien, Courret, Laurens, & Dartus, 2014; Lacey & Rennie, 2012). Low-velocity regions, and associated flow features, were observed and taken advantage of by the fish (David, Calluaud, Pineau, & Texier, 2012; Johnson & Rice, 2014). New evidences on the role of roughness are sometimes conflicting. Although several studies associated upstream navigability of certain fish species with an increase in roughness (e.g., Heaslip, 2015), others reported minimum benefit to fish swimming performance (e.g., Nikora, Aberle, Biggs, Jowett, & Sykes, 2003). Despite these inconsistencies, the common view remains that low-velocity zones (LVZs) such as sidewalls and corners are favoured by fish (Cotel, Webb, & Trittico, 2006; Lupandin, 2005), as confirmed by recent observations with small-bodied fish (Cabonce, Fernando, Wang, & Chanson, 2017; Wang & Chanson, 2018b; Wang, Chanson, Kern, & Franklin, 2016).

Culvert barrel baffles have been reviewed extensively as an alternative to reduce excessive barrel velocities to improve fish passage (Chanson & Uys, 2016; Duguay & Lacey, 2014; Larinier, 2002; Olsen & Tullis, 2013; Rajaratnam, Katapodis, & Dodewuk, 1991). In most applications, baffles may drastically decrease the hydraulic capacity of culverts for a range of discharges (Larinier, 2002; Olsen & Tullis, 2013). A small corner baffle system tested by Cabonce et al. (2017) was successful at improving upstream passage for small-bodied fish during less-than-design events. Alternatively, an asymmetrically roughened culvert barrel may be considered (Wang, Beckingham, Johnson, Kiri, & Chanson, 2016; Wang, Chanson, et al., 2016). Importantly, the reconciliation between the economic and ecological aspects of culvert design remains a most significant challenge to this day (Fairfull & Witheridge, 2003; Hunt, Clark, & Tkach, 2012).

Fish behaviours are understood to be influenced by the surrounding hydrodynamic environment (Papanicolaou & Talebbeydokhti, 2002). A target fish species may react to surrounding turbulent structures and secondary flow patterns while navigating. As such, a comprehensive understanding of fish navigability in culverts requires examinations of both mean and turbulent flow patterns in three dimensions. Properly validated computational fluid dynamics (CFDs) models provide a means to reveal the fundamental processes driven by each culvert configuration, and offers improved data fidelity as well as level of description while keeping the study cost moderate (Hotchkiss, 2002; Nikora et al., 2003; Pavlov, Lupandin, & Skorobogatov, 2000). CFD models have been successfully applied to investigations of baffled culvert hydrodynamics by Feurich, Boubee, and Olsen (2012) and Khodier and Tullis (2017).

The aim of the present study is to understand how different types of box culvert designs benefit upstream passage of small-bodied fish using RANS- and LES-based three-dimensional CFD models. Boundary configurations including smooth walls, rough bed and left sidewall, and small corner baffles were examined. The study pertains to small-bodied Australian native species, where prior testing was undertaken with juvenile silver perch (*Bidyanus bidyanus*) and Duboulay's rainbowfish (*Melanotaenia duboulayi*). The results reveal fundamental flow processes that may affect fish navigability and provide guidance to future culvert barrel baffle designs.

2 | NUMERICAL METHODS

2.1 | Theory

Box culvert hydrodynamics represent a broad spectrum of turbulent motions with dimensions ranging from the internal barrel width down to the Kolmogorov scale. Interactions between turbulent features result in unique flow patterns for each boundary configuration and discharge. Flow complexities due to geometry and transitory behaviours can be resolved comprehensively for better examination of their relevance to upstream fish passage. Herein, computations were performed using a commercial package, ANSYS Fluent v18.0, on a Dell™ Precision T5810 workstation equipped with a Xeon® E5-1680v4 processor and 128 GB random-access memory.

The numerical models resolve the flow field by solving the governing continuity and momentum equations for a steady, incompressible flow:

$$\frac{\partial u_i}{\partial x_i} = 0, \tag{1}$$

$$\frac{\partial u_i}{\partial t} + u_j \frac{\partial u_i}{\partial x_j} = g_i - \frac{1}{\rho}\frac{\partial p_i}{\partial x_i} + \frac{\partial \tau_{ij}}{\partial x_j}, \tag{2}$$

where u_i is the velocity component in the direction of x_i (i = 1, 2, 3), t is time, g_i is the gravity component in the direction of x_i, ρ is the fluid density, and p_i and τ_{ij} are the isotropic and deviatoric stress components, respectively. Additionally, the free surface may be trackable using a volume of fluid method by solving a transport equation (Hirt & Nichols, 1981):

$$\frac{\partial \alpha}{\partial t} + u_j \frac{\partial \alpha}{\partial x_j} = 0, \tag{3}$$

where an interface exists for $0 < \alpha < 1$. The interface orientation is determined by the surface normal computed from α.

The present study considered a single culvert barrel cell and three-barrel configurations were tested: smooth, asymmetrically roughened, and corner baffled. The selection of turbulence model depends on the desired level of description, barrel geometry, and flow characteristics. The simplest k-ε model was applied to the smooth barrel due to its geometrical simplicity. This model is widely incorporated into most CFD codes and is well validated for two-dimensional thin shear flow with small pressure gradient (Pope, 2000). For the asymmetrically roughened barrel, the flow redistribution is governed by secondary circulations, which the k-ε model was unable to reproduce. The Reynolds stress model overcomes this limitation by solving for all components of turbulent stress and was hence adopted for simulating this configuration. The last configuration featuring triangular corner baffles produces a time-dependent flow field, which requires simulation be performed in a correspondent manner. Consequently, a wall modelled large-eddy simulation was adopted to recover the time-dependent behaviours of the most important turbulent structures without being prohibitively demanding on computational resources (Rodi, Constantinescu, & Stoesser, 2013).

The model geometries were incorporated into the software using a combination of structured and unstructured hexahedral blocks. The cells were distributed following the rules below, where possible:

- Free surface remains (mostly) orthogonal to the cell boundaries;
- Smaller cells are applied to important regions (e.g., behind baffle), including boundaries and geometric transitions;
- Structured mesh is used when possible;
- Dense mesh is preferred if computational time remains manageable.

Details of the CFD simulations are summarized in Tables 1–3.

TABLE 1 Computational fluid dynamic configurations for smooth channel

Item	Configuration	Notes
Geometry	9.35 × 0.5 × 1.0 m^3	Length × Width × Height
Mesh	500 × 25 × 100	1,287,500 cells, hexahedral
Model	Transient k-ε	Default coefficients
Top boundary	Symmetry	—
Bottom boundary	Wall	k_s = 1.5 × 10^{-6} m
Side boundaries	Wall	k_s = 1.5 × 10^{-6} m
Inlet type	Velocity	$U_{w,in}$ = 0.5645 ms^{-1}
Solution	Coupled/2nd order	—

2.2 | Validation

For all configurations, the numerical results were compared with the detailed experimental observations of Wang, Beckingham, et al. (2016); Cabonce et al. (2017); and Cabonce, Wang, and Chanson (2018). Detailed validation of each model is reported in Zhang and Chanson (2018). The free-surface profiles between numerical and experimental data agreed within 10%. Agreement for velocity profiles was typically 10% for the smooth channel and 20% for the asymmetrically roughened and baffled channels. All numerical models produced consistent cross-sectional flow distributions with the experimental data and were able to replicate the most important features (e.g., secondary flow and recirculation) associated with each culvert configuration. The results suggested that the present models are reliable for simple geometries and are useful as complementary tools to explain complex flow behaviours encountered in physical studies. Complementary fish testings were undertaken by Wang, Chanson, et al. (2016), Cabonce et al. (2017), and Cabonce et al. (2018), and the flow features that were observed to influence fish behaviours were identifiable within the CFD results.

3 | HYDRODYNAMICS OF BOX CULVERT BARREL

3.1 | Presentation

Three types of culvert barrel geometries were simulated (Table 4). Table 4 summarizes each numerically tested configuration. Further details are reported in Zhang and Chanson (2018). The reference case study is a 12-m long, 0.5-m wide rectangular channel, corresponding to a single cell culvert beneath a small two-lane countryside road. Detailed water level and velocity data were provided by Wang, Beckingham, et al. (2016). This configuration represents the typical operating scenario for which no special provisions are made for fish passage.

The second configuration includes a very-rough invert, a very-rough left sidewall, and a smooth right sidewall, in the same 12-m long 0.5-m wide channel. The concept was proposed and tested by Wang, Beckingham, et al. (2016) to characterize asymmetrical boundary roughness as a remedial measure to assist upstream fish passage for less-than-design flows. The roughness asymmetry induces a favoured swimming zone for fish and could be relatively easily implemented on existing box culverts.

TABLE 2 Computational fluid dynamic configurations for channel with rough bed and left sidewall

Item	Configuration	Notes
Geometry	12.0 × 0.5 × 0.5 m^3	Length × Width × Height
Mesh	500 × 100 × 100	5,000,000 cells, hexahedral
Model	Transient RSM	Default coefficients
Top boundary	Symmetry	—
Bottom boundary	Wall	k_s = 2.0 × 10^{-2} m
Side boundaries	Wall	k_s = 2.0 × 10^{-4} m
Inlet type	Velocity	Profile from Wang, Beckingham, et al. (2016)
Solution	SIMPLE/2nd order	—

Note. RSM: Reynolds stress model.

TABLE 3 Computational fluid dynamic configurations for channels with corner baffles

Item	Configuration	Notes
Geometry	Varies	—
Mesh	Varies	300,000–705,000 cells, hexahedral
Model	WMLES	Default coefficients
Top boundary	Symmetry	—
Bottom boundary	Wall	—
Side boundaries	Wall	—
Inlet type	Periodic	Mass flow rate fixed
Solution	SIMPLE/2nd order	—

Note. WMLES: wall modelled large-eddy simulation.

TABLE 4 Summary of channel configurations

Type	Q (m^3/s)	Channel details	Turbulence model
Smooth	0.0556	L = 12 m, W = 0.50 m, k_s = 1.5 × 10^{-6} m	k-ε + VOF
Rough bed/left sidewall	0.0556	L = 12 m, W = 0.478 m, k_s = 2 × 10^{-2} m	RSM + VOF
Triangular corner baffle	0.0264	L = 12 m, W = 0.50 m, h_b = 0.067 m, L_b = 0.67 m, d = 0.1 m	LES
	0.0556	L = 12 m, W = 0.50 m, h_b = 0.067 m, L_b = 0.67 m, d = 0.165 m	LES
	0.0556	L = 12 m, W = 0.50 m, h_b = 0.133 m, L_b = 0.67 m, d = 0.173 m	LES
	0.0556	L = 12 m, W = 0.50 m, h_b = 0.133 m, L_b = 0.67 m, d = 0.173 m, Ø 13-mm hole	LES

Note. h_b: triangular baffle size; k_s: equivalent sand roughness height; L: barrel length; L_b: triangular baffle longitudinal spacing, Q: water discharge; RSM: Reynolds stress model; VOF: volume of fluid; W: internal barrel width.

The last configuration consist of small triangular corner baffle system installed along the left bottom corner of the 12-m long 0.5-m wide channel. The system was recently introduced (Cabonce et al., 2017; Carbonce et al., 2018; Chanson & Uys, 2016) and has been shown successfully to have minimum impact on flood capacity at design discharge, while improving endurance for small-bodied fish for less-than-design discharges. The effectiveness of the system primarily depends on the relative spacing between baffles, that is, L_b/h_b where L_b is the longitudinal spacing and h_b is the baffle size, and the baffle submergence h_b/d, where d is the water depth. Four variants of the baffle system were tested to identify their hydraulic differences and potential implications for fish (Table 4).

3.2 | Velocity results

Numerical calculations were performed for the flow and boundary conditions listed in Table 4. For each set of calculations, detailed laboratory data were available. Figures 1 and 2 present typical results that are discussed below. Further comparative results were discussed by Zhang and Chanson (2018).

Figure 1a presents the simulated longitudinal velocity contours (U) for the barrel with rough bed and left sidewall (y = 0.5 m), where y and z are the spanwise and normal coordinates, respectively. Compared with the smooth barrel (data not shown), the roughness asymmetry results in skewed velocity contours with a sizeable low-velocity zone next to the rough sidewall (y = 0.5 m) and an associated increase in free surface level. Further inspection reveals approximately 40% of flow area with less than the bulk velocity, that is, U/U_{mean} < 1, comparable with detailed laboratory observations (Wang, Beckingham, et al., 2016). The observed increase in flow depth and decrease in velocity on the rough side are both perceived as conducive to fish passage. Figure 2b shows the spanwise distributions of maximum streamwise velocity (U_{max}), characterizing the flow redistribution initiated by the boundary configuration. Although some disparity exists between the

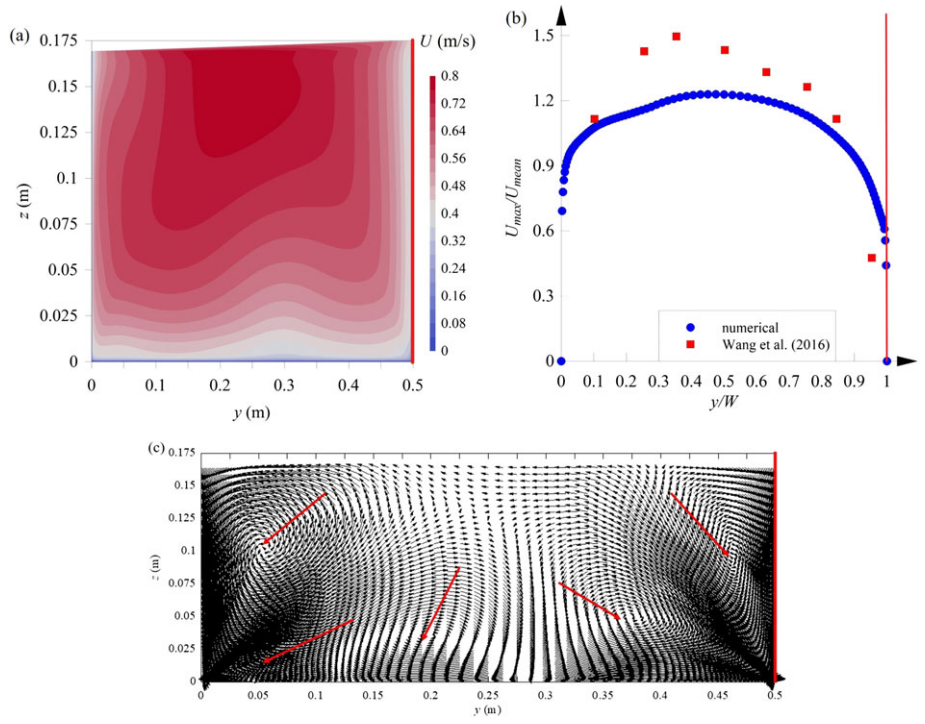

FIGURE 1 Velocity field in culvert barrel with rough bottom and rough left sidewall (k ≈ 20 mm). (a) Simulated longitudinal velocity contours (U). (b) Distribution of characteristic maximum streamwise velocity within a cross section—comparison between computational fluid dynamic numerical data and physical data (Wang, Beckingham, et al., 2016). (c) Simulated secondary flow patterns in barrel with rough bottom and left. Flow conditions: Q = 0.055.6 m^3/s, W = 0.5 m, d = 0.165 m. Rough sidewall on the right-hand side of graphs [Colour figure can be viewed at wileyonlinelibrary.com]

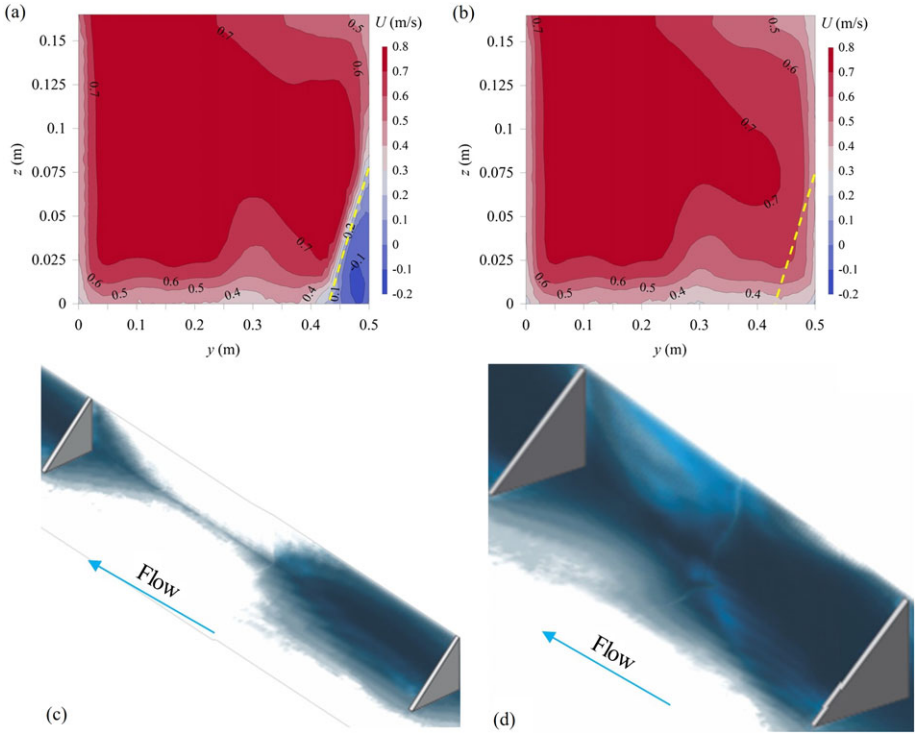

FIGURE 2 Simulated velocity field and low-velocity zones (LVZs) in culvert barrel with small triangular corner baffle on one side: (a) h_b = 0.067 m, L_b = 0.67 m, $(x - x_b)/L_b$ = 0.05; (b) h_b = 0.067 m, L_b = 0.67 m, $(x - x_b)/L_b$ = 0.765; (c) LVZ where U/U_{mean} < 0.5 for h_b = 0.067 m, L_b = 0.67 m; (d) LVZ where U/U_{mean} < 0.5 for h_b = 0.133 m, L_b = 0.67 m. Flow conditions: Q = 0.055.6 m^3/s, W = 0.50 m, $d \approx$ 0.165 m. LVZ defined as U/U_{mean} < 0.5. Darker shades correspond to lower velocity [Colour figure can be viewed at wileyonlinelibrary.com]

two datasets, both results indicate a smaller maximum velocity next to the left rough sidewall (y/W = 1). This is advantageous to the fish as a single continuous LVZ, that is, in corner of rough bed and sidewall, is more traversable than two smaller LVZs occupying the corners of a typical smooth barrel.

The lateral perturbation induced by the channel corners and boundary roughness leads to the formation of secondary currents (Nezu, Nakagawa, & Jirka, 1994; Nezu & Rodi, 1986), which are responsible for dips in velocity contours (Figure 1a). Figure 1c illustrates the computed secondary flow patterns in the asymmetrically roughened barrel, where obvious recirculation cells are marked with red arrows. The computed secondary flow pattern generally matches that visualized by Wang, Beckingham, et al. (2016) using dye injection. Pairs of counter-rotating corner eddies and a supersized eddy occupying approximately 40% of the flow width are identified above the invert. The confluence between this eddy and another smaller recirculation next to the rough wall is responsible for significant velocity reductions next to y = 0.3 m (Figure 1a), which may provide additional benefit to fish navigation.

Typical longitudinal velocity contours in the corner baffle configurations are shown in Figure 2a. The data are presented immediately downstream (Figure 2a) and upstream (Figure 2b) of the small corner baffle. The numerical results were sampled over 10 s at 1000 Hz. The corner baffle heavily disturbs the surrounding flow field and creates a recirculating zone in its immediate wake (Figure 2a). Negative velocities up to −0.2 m/s are recorded, which may disorient small-body fish with low endurance speeds, as reported by Cabonce et al. (2018). The recirculation zones typically extend up to three times the baffle size, after which a globally positive velocity field is restored (Figure 2b). Generally, the corner baffles produce much larger LVZs than the smooth and asymmetrically roughened barrels, although the large streamwise velocity variation behind baffles may create disconnected regions that adversely affect fish passage.

Selecting the appropriate baffle size reflects a trade-off between reducing the hydraulic capacity of the culvert and providing adequate passage for the fish. Maximum benefit is available when the baffle size is comparable with the fish size, and small relative to the flow depth (i.e., optimized for less-than-design flow conditions). Closer baffle-to-baffle spacings reduce the streamwise flow variation and in turn improve the connectivity between LVZs, which benefits fish navigation. Other strategies to reduce flow reversal include using perforated baffles (Cabonce et al., 2018), though the present study found limited benefit provided by a Ø 13-mm opening through the baffle centroid.

4 | CHARACTERIZATION OF LVZs

LVZs are swimming zones favoured by fish (Cotel et al., 2006). In particular, small-bodied fish, with characteristic endurance speed less than 0.6 m/s, prefer to swim next to walls and in corners during upstream passage (Cabonce et al., 2017; Wang, Chanson, et al., 2016). The finding may be explained in terms of their rates of work and energy expended in thrust during swimming. For upstream passage, the rate of work is proportional to the cube of the local longitudinal velocity U^3 (Wang & Chanson, 2018a). An accurate assessment of LVZs requires a complete characterization of flow evolution

through cross sections, in relation to fish swimming observations. In this section, validated CFD results are used to provide a global characterization of LVZs associated with each roughness configuration, corresponding to typical less-than-design flow conditions.

Fish navigability within a channel depends upon the size, location, and connectivity of the LVZs. Contiguous LVZs forming a long stretch of sizeable flow area is naturally more traversable than scattered LVZs of smaller sizes. Consequently, maximizing LVZ cross-section areas and minimizing streamwise variations in these zones are keys to minimize energy expenditure and to facilitate upstream fish passage. Figure 3a,b present three-dimensional visualizations of the LVZs generated in the smooth (Figure 3a) and asymmetrically roughened (Figure 3b) channels at the same discharge, where the main flow direction is from bottom right to top left. The visualizations were obtained by directly rendering the CFD results in the fully developed flow region. Areas with less than 50% of the bulk velocity (i.e., U/U_{mean} < 0.5) are shaded in blue and considered as proxy of LVZs. Darker shades are associated with larger LVZ area and potentially preferred upstream passage routes. In the smooth channel, the only traversable areas are the small corner regions, which are identically sized because the channel is symmetrical. For a number of small-bodied fish, passage may be difficult because the low-velocity regions are too small and lie close to the physical boundaries. The rough bed and left sidewall configuration results show a preferential passage towards the rough sidewall, where the LVZ occupies a larger area than on the smooth side. Additionally, an LVZ is identified on the bottom at a slight offset from the channel centreline where two large secondary flow cells meet. Figure 3c,d compare the fraction of flow area where U/U_{mean} < 1 for both smooth and rough barrel channels. Despite some differences, the experimental and numerical results exhibit a high degree of consistency, with a correlation coefficient of 0.942 and a standard error of 0.072. In Figure 3c,d, the vertical axis represents the proportion of flow cross-sectional area with U/U_{mean} less than the given value on the horizontal axis. Although both smooth and rough boundary configurations experience at least 30% of the flow area with U/U_{mean} < 1, their abilities to provide regions with lower longitudinal velocities, that is, U/U_{mean} < 0.75 and U/U_{mean} < 0.5, diverge drastically. The rough boundary channel exhibits a clear advantage over the smooth flume for U/U_{mean} < 0.75 (Figure 3d).

Considering the channel equipped with small corner baffles, Figure 2c,d illustrate LVZ developments, for the same discharge, but for two different baffle sizes (h_b = 0.066 and 0.133 m). Only areas with U/U_{mean} < 0.5 are rendered. For both cases, LVZs are produced in the baffle wake and immediately upstream of the baffle. The latter LVZ is induced by some flow stagnation on the upstream face of the baffle and was found to be a most efficient rest area for small-bodied fish propagating upstream (Cabonce et al., 2018). Altogether, the LVZs produced by the smallest baffles (Figure 2c) diminish rapidly with distance downstream of the baffle, and there is a lack of streamwise connectivity between LVZs, which would be detrimental to upstream fish passage. The reduction in LVZ size could be compensated by selecting a larger baffle size (Figure 2c) that increases the rate of energy dissipation and reduce the discharge capacity of the structure. Furthermore, larger baffles may induce strong flow recirculation, which may disorient a number of small fish (Cabonce et al., 2017). This is a major limitation of the corner baffle design, although that baffle ventilation strategies might be considered to alleviate the disorienting effect of baffles on small-bodied fish species (Cabonce et al., 2018).

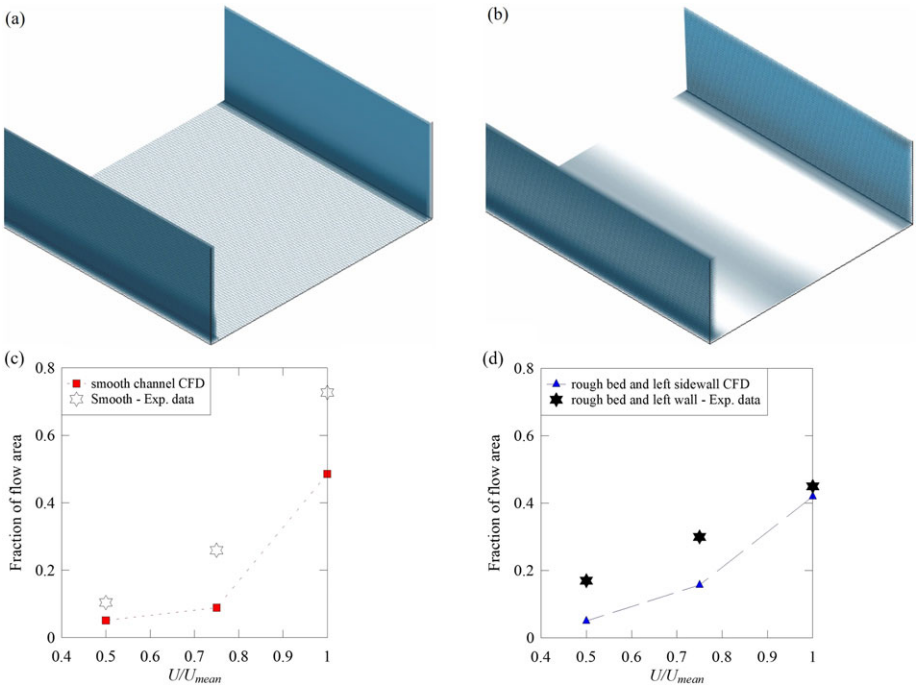

FIGURE 3 Simulated low-velocity zones (LVZs) for smooth channel and channel with rough bed and left sidewall. (a) LVZ in smooth channel. (b) LVZ in channel with rough bed and left sidewall. (c) LVZ fraction of total flow area in smooth channel. (d) LVZ fraction of total flow area in channel with rough bed and left sidewall. Flow conditions: Q = 0.0556 m^3/s, W = 0.5 m. Experimental data from Wang, Beckingham, et al. (2016). LVZ defined as U/U_{mean} < 0.5. Darker shades correspond to lower velocity. CFD: computational fluid dynamic [Colour figure can be viewed at wileyonlinelibrary.com]

5 | CONCLUSION

Three-dimensional CFD simulations were performed to compare the effectiveness of different box culvert barrel configurations on upstream fish passage, for less-than-design flow conditions. The hydrodynamic behaviours of smooth, asymmetrically roughened, and baffled barrels were examined. The results provided insights into the relevance of boundary configurations to fish passage and might offer guidance for future design optimizations.

LVZ illustrations demonstrated that asymmetric roughness and comer baffles may improve fish navigability in relation to a standard smooth barrel in distinguishing ways. Cross-sectional flow asymmetry and streamwise contiguity of low-velocity regions were identified as desirable geometric traits to benefit the generation of large, contiguous LVZs suitable for upstream fish passage. Corners, confluence of secondary flow cells, and direct obstructions were contributing factors to LVZ production. Future fish-friendly culvert designs should incorporate these features and consider optimization for a wider range of discharges.

Validation of CFD models against laboratory studies under carefully controlled flow conditions demonstrated the adequacy and effectiveness of CFD usage to assess effects of changes to cross-sectional shape and boundary configuration. The use of CFD models is recommended in complement of laboratory physical studies to explain mechanisms responsible for field observations. Importantly, complete and detailed physical datasets are always essential to CFD as no "experimental data means no validation" (Chanson & Lubin, 2010; Roache, 2009).

ACKNOWLEDGEMENTS

The authors thank Dr. Hang Wang for helpful discussions. The financial support of Australian Research Council (Grant LP140100225) is acknowledged.

DECLARATION OF INTEREST

The authors have no financial interest or benefit that has arisen from the direct applications of the research.

ORCID

Gangfu Zhang http://orcid.org/0000-0002-3368-7326
Hubert Chanson http://orcid.org/0000-0002-2016-9650

REFERENCES

Baki, A. B., Zhu, D. Z., & Rajaratnam, N. (2014). Mean flow characteristics in a rockramp-type fish pass. *Journal of Hydraulic Engineering*, *140*(2), 156–168.

Behlke, C. E., Kane, D. L., Mcleen, R. F., & Travis, M. T. (1991). Fundamentals of culvert design for passage of weak-swimming fish. Report FHW A-AK-RD-90-10, Department of Transportation and Public Facilities, State of Alaska, Fairbanks, USA, 178 pp.

Cabonce, J., Fernando, R., Wang, H., & Chanson, H. (2017). Using triangular baffles to facilitate upstream fish passage in box culverts: Physical modelling. Report 107/17, School of Civil Engineering, The University of Queensland, Australia, 132 pp.

Cabonce, J., Wang, H., & Chanson, H. (2018). Ventilated corner baffles to assist upstream passage of small-bodied fish in box culverts. *Journal of Irrigation and Drainage Engineering*, *ASCE*, *144*(8), Paper 0418020, 8. https://doi.org/10.1061/(ASCE)IR.1943-4774.0001329

Cassan, L., Tien, T. D., Courret, D., Laurens, P., & Dartus, D. (2014). Hydraulic resistance of emergent macroroughness at large Froude numbers: Design of nature-like fishpasses. *Journal of Hydraulic Engineering*, *140*, 9, 04014043.

Chanson, H. (2000). Introducing originality and innovation in engineering teaching: The hydraulic design of culverts. *European Journal of Engineering Education*, *25*(4), 377–391. https://doi.org/10.1080/03043790050200421

Chanson, H. (2004). *The hydraulics of open channel flow: An introduction* (2nd ed.). (p. 630). Oxford, UK: Butterworth-Heinemann.

Chanson, H., & Lubin, P. (2010). Discussion of verification and validation of a computational fluid dynamics (CFD) model for air entrainment at spillway aerators. *Canadian Journal of Civil Engineering*, *37*(1), 135–138. https://doi.org/10.1139/L09-133

Chanson, H., & Uys, W. (2016). Baffle designs to facilitate fish passage in box culverts: A preliminary study. *Proc. 6th IAHR International Symposium on Hydraulic Structures*, Portland, OR, USA, pp. 295-304 doi: 10.15142/T300628160828.

Chorda, J., Larinier, M., & Font, S. (1995). Le Franchissement par les Poissons Migrateurs des Buses et Autres Ouvrages de Rétablissement des Ecoulements Naturels lors des Aménagements Routiers et Autoroutes. Etude Expérimentale. Rapport HYDRE n°159 -GHAAPPE n°95-03, Groupe d'Hydraulique Appliquée aux Aménagements Piscicoles et à la Protection de l'Environnement, Service d'Etudes Techniques des Routes et Autoroutes, Toulouse, France, 116 pp (in French).

Cotel, A. J., Webb, P. W., & Trittico, H. (2006). Do brown trout choose locations with reduced turbulence? *Transactions of the American Fisheries Society*, *135*, 610–619.

David, L., Calluaud, D., Pineau, G., & Texier, A. (2012). Fishway hydrodynamics and global approaches for insuring the upstream migration around dams. *Proc. 4th IAHR International Symposium on Hydraulic Structures*, Porto, Portugal, 15 pp. (CD-ROM).

Duguay, J., & Lacey, R. W. J. (2014). Effect of fish baffles on the hydraulic roughness of slip-lined culverts. *Journal of Hydraulic Engineering*, *141*(1), 10. https://doi.org/10.1061/(ASCE)HY.1943-7900.0000942

Fairfull, S., & Witheridge, G. (2003). *Why do fish need to cross the road? Fish passage requirements for waterway crossings*. (p. 14). Cronulla NSW, Australia: NSW Fisheries.

Feurich, R., Boubee, J., & Olsen, N. R. B. (2012). Improvement of fish passage in culverts using CFD. *Ecological Engineering*, *47*, 1–8.

Heaslip, B. M. (2015). Substrate roughening improves swimming performance of two small bodied riverine fish species: Implications for culvert design. Honours Thesis, School of Biological Sciences, The University of Queensland, Brisbane, Australia, 32 pp.

Herr, L. A., & Bossy, H. G. (1965). Hydraulic charts for the selection of highway culverts. *Hydraulic Engineering Circular*, US Dept. of Transportation, Federal Highway Admin., HEC No. 5, December.

Hirt, C., & Nichols, B. (1981). Volume of fluid (VOF) method for the dynamics of free boundaries. *Journal of Computational Physics*, *39*(1), 201–225.

Hotchkiss, R. (2002). Turbulence investigation and reproduction for assisting downstream migrating juvenile salmonids, part I. BPA report DOE/BP-00004633-I, Bonneville Power Administration, Portland, Oregon, 138 pp.

Hotchkiss, R. H., & Frei, C. M. (2007). Design for fish passage at roadway-stream crossings: Synthesis report. Publication no. FHWA-HIF-07-033, Federal Highway Administration, US Department of Transportation, 280 pp.

Hunt, M., Clark, S., & Tkach, R. (2012). Velocity distributions near the inlet of corrugated steel pipe culverts. *Canadian Journal of Civil Engineering*, *39*, 1243–1251.

Hurst, T. P., Kay, B. H., Ryan, P. A., & Brown, M. D. (2007). Sublethal effects of mosquito larvicides on swimming performance of larvivorous fish *Melanotaenia duboulayi* (Atheriniformes: Melanotaeniidae). *Ecotoxicology*, *100*(1), 61–65.

Johnson, M. F., & Rice, S. P. (2014). Animal perception in gravel-bed rivers: Scales of sensing and environmental controls on sensory information. *Canadian Journal of Fisheries and Aquatic Sciences*, *71*, 945–957.

Khodier, M., & Tullis, B. (2017). Experimental and computational comparison of baffled-culvert hydrodynamics for fish passage. *Journal of Applied Water Engineering and Research*, 1–9.

Lacey, R. W. J., & Rennie, C. D. (2012). Laboratory investigation of turbulent flow structure around a bed-mounted cube at multiple flow stages. *Journal of Hydraulic Engineering*, *138*(1), 71–84.

Larinier, M. (2002). Fish passage through culverts, rock weirs and estuarine obstructions. *Bulletin Français de Pêche et Pisciculture*, *364*(18), 119–134.

Lupandin, A. I. (2005). Effect of flow turbulence on swimming speed of fish. *Biology Bulletin*, *32*(5), 461–466.

Nezu, I., Nakagawa, H., & Jirka, G. H. (1994). Turbulence in open-channel flows. *Journal of Hydraulic Engineering*, *120*(10), 1235–1237.

Nezu, I., & Rodi, W. (1986). Open-channel flow measurements with a laser Doppler anemometer. *Journal of Hydraulic Engineering*, *112*(5), 335–355.

Nikora, V., Aberle, J., Biggs, B., Jowett, I., & Sykes, J. (2003). Effects of fish size, time-to-fatigue and turbulence on swimming performance: A case study of Galaxias maculatus. *Journal of Fish Biology*, *63*, 1365–1382.

Olsen, A., & Tullis, B. (2013). Laboratory study of fish passage and discharge capacity in slip-lined, baffled culverts. *Journal of Hydraulic Engineering*, *139*(4), 424–432.

Papanicolaou, A .N., & Talebbeydokhti, N. (2002). Discussion of "Turbulent open-channel flow in circular corrugated culverts." *Journal of Hydraulic Engineering*, *128*(5), 424–432.

Pavlov, D. S., Lupandin, I. A., & Skorobogatov, M. A. (2000). The effects of flow turbulence on the behaviour and distribution of fish. *Journal of Ichthyology*, *40*, S232–S261.

Pope, S. B. (2000). *Turbulent flows*. Cambridge University Press.

Rajaratnam, N., Katapodis, C., & Dodewuk, S. (1991). Hydraulics of culvert fishways IV: Spoiler baffle culvert fishways. *Canadian Journal of Civil Engineering*, *18*, 76–82.

Roache, P. J. (2009). Perspective: Validation—What does it mean? *Journal of Fluids Engineering*, *131*, 4, 034503.

Rodgers, E. M., Cramp, R. L., Gordos, M., Weier, A., Fairfull, S., Riches, M., & Franklin, C. E. (2014). Facilitating upstream passage of small-bodied fishes: Linking the thermal dependence of swimming ability to culvert design. *Marine and Freshwater Research*, *65*, 710–719. https://doi.org/10.1071/MF13170

Rodi, W., Constantinescu, G., & Stoesser, T. (2013). *Large-eddy simulation in hydraulics*. (p. 252). Leiden, The Netherlands: IAHR Monograph, CRC Press, Taylor & Francis Group.

Wang, H., Beckingham, L. K., Johnson, C. Z., Kiri, U. R., & Chanson, H. (2016). Interactions between large boundary roughness and high inflow turbulence in open channel: A physical study into turbulence properties to enhance upstream fish migration. Hydraulic model report no. CH103/16, School of Civil Engineering, The University of Queensland, Brisbane, Australia, 74 pp. (ISBN 978-1-74272-156-9).

Wang, H., & Chanson, H. (2018a). Modelling upstream fish passage in standard box culverts: Interplay between turbulence, fish kinematics, and energetics. *River Research and Applications*, *34*(3), 244–252. https://doi.org/10.1002/rra.3245

Wang, H., & Chanson, H. (2018b). On upstream fish passage in standard box culverts: Interactions between fish and turbulence. *Journal of Ecohydraulics*, *3*(1) IAHR. doi: https://doi.org/10.1080/24705357.2018.1440183). (In print)

Wang, H., Chanson, H., Kern, P., & Franklin, C. (2016). Culvert hydrodynamics to enhance upstream fish passage: Fish response to turbulence. *Proc. 20th Australasian Fluid Mechanics Conference*, Perth WA, Australia, 5-8 December, Paper 682, 4 pp.

Zhang, G., & Chanson, H. (2018). Numerical investigations of box culvert hydrodynamics with smooth, unequally roughened and baffled barrels to enhance upstream fish passage. Hydraulic model report no. CH111/18, School of Civil Engineering, The University of Queensland, Brisbane, Australia, 129 pp.

How to cite this article: Zhang G, Chanson H. Three-dimensional numerical simulations of smooth, asymmetrically roughened, and baffled culverts for upstream passage of small-bodied fish. *River Res Applic*. 2018;34:957–964. https://doi.org/10.1002/rra.3346